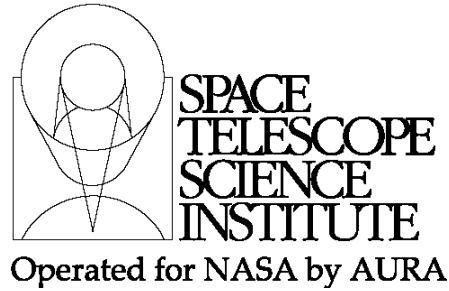




TECHNICAL REPORT



Title: Mid-Infrared Instrument (MIRI) Low Resolution Target Acquisition for Faint Sources	Doc #: JWST-STScI-001347 SM-12 Date: 3 April 2008 Rev:
Authors: Karl Gordon Phone: 410-338-5031	Release Date: 11 April 2008

1.0 Abstract

Target acquisition for MIRI Low Resolution Slit Spectroscopy (LRS-Slit) of faint sources can be done using long exposures (e.g. 1000 sec) on the faint source itself, but requires an enhanced method for the slope image creation to remove the numerous cosmic rays. The required accuracy for placing a source in the LRS slit aperture is 20 mas. The centroid of a source must be measured to 5 mas to ensure that the accuracy of the required spacecraft move is close to 20 mas. The faintest source for which a 5 mas or better centroid can be measured in 960 sec using the enhanced method was determined using simulations to be 2.7, 25, and 288 μ Jy for the F560W, F1000W, and F1500W filters, respectively. It is not possible to measure a 5 mas or better centroid with the F2550W filter.

2.0 Introduction

One of the capabilities of the Mid-Infrared Instrument (MIRI) on JWST is low resolution long-slit spectroscopy from 5-10 μ m. This instrument mode is likely to be used for spectroscopy of very faint sources in regions of the sky that lack nearby bright sources (e.g., cosmological deep fields). The lack of nearby bright sources is compounded by the need to accurately know the offset between the bright source and faint target source. In addition, the nearby bright source would have to be within approximately 60" to be able to use the same guide star. Thus, it is expected that target acquisition on faint sources will be desired for this mode. The baseline is for target acquisitions on faint sources with exposure times up to ~1000 seconds. The limit of 1000 seconds is not a hard limit, but reasonable given the conservative expectation that around 50% of the pixels will be affected by a cosmic ray in this exposure time. In addition, if a source is not bright enough to use for centroiding in 1000 seconds, it is unlikely to produce a useful LRS-Slit spectrum in a reasonable amount of time. Given these long exposures, cosmic rays will be a significant issue as they are predicted to affect ~50% of the pixels in 1000 sec exposures. An on-board, efficient, and accurate cosmic ray removal algorithm is required for target acquisition for these long exposures. The low resolution slit has dimensions of 5.5"x0.6" and requires positioning the source in the slit with an accuracy of 20 mas to stay within the error budget for wavelength calibration (Glasse 2006). The target

Operated by the Association of Universities for Research in Astronomy, Inc., for the National Aeronautics and Space Administration under Contract NAS5-03127

Check with the JWST SOCCER Database at: <http://soccer.stsci.edu/DmsProdAgile/PLMServlet>
To verify that this is the current version.

acquisition will be done using an adjacent portion of the MIRI imager using a small angle maneuver that will introduce a 20 mas uncertainty.

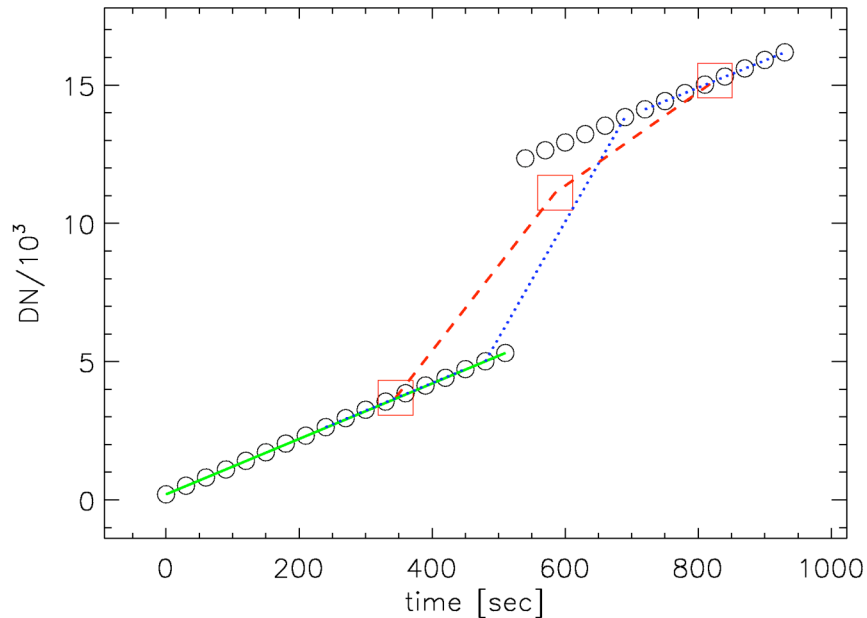


Figure 1: The different methods of estimating the slope measurement for a long integration on board JWST are shown. The open circles given the frames in a simulated MIRI integration on a single pixel with a cosmic ray near the middle of the integration. The red squares show the mega-frames and the red dashed line the slope estimates used as part of the modified method. The blue dotted lines show the slope estimates used as part of the enhanced method. The green solid line shows the full method.

3.0 Simulations

Simulations of long MIRI imaging exposures were carried out to quantitatively assess different algorithms for cleaning cosmic rays from the target acquisition images. The quantitative goal of the simulations is to be able to determine the centroid of a point source with an accuracy that does not affect the wavelength or flux calibration of the resulting spectrum. This corresponds to a 1-sigma uncertainty in the spacecraft move plus centroiding accuracy of 20 milliarcsec (mas) and is set to stay within the 1.0% error budget for wavelength calibration (Glasse 2006). This requires a centroid accuracy of 5 mas to have the centroid uncertainty a negligible contribution to the total 1-sigma uncertainty.

Check with the JWST SOCCER Database at: <http://soccer.stsci.edu/DmsProdAgile/PLMServlet>
To verify that this is the current version.

Table 1: Wavelength/Filter Dependent Parameters

	F560W	F1000W	F1500W	F2550W
Sky/Telescope background [e/sec/pixel]	6.76	93.7	493	8280
Source FWHM [arcsec]	0.2	0.35	0.53	0.9
Source [(e/sec)/mJy]	1.2×10^4	1.6×10^4	1.8×10^4	8.5×10^3

The simulations consisted of creating image cubes with dimensions of 32x16x32. These image cubes represent a 32x32 pixel region of the MIRI imager and an exposure of 960 seconds non-destructively sampled every 30 sec (i.e., 32 frames). The MIRI imager has a plate scale of 0.11 arcsec/pixel.

Each pixel ramp includes contributions and noise from dark current, read noise, sky/telescope background, and source flux. The dark current is set to 0.3 e/sec which is much smaller than sky background. The read noise is 19 e per 30 sec frame. The sky background depends on the observation wavelength (i.e., filter). The source PSF depends on wavelength as well and is approximated as a 2D Gaussian. The sky/telescope and source wavelength dependent parameters are given in Table 1 and are mainly taken from G. Rieke's radiometric model spreadsheets.

Cosmic rays were inserted into the simulations assuming a delta function hit amplitude of 20,000 electrons (3,356 DN). The probability of a cosmic ray hitting a pixel was assumed to be $5 \times 10^{-4} \text{ sec}^{-1} \text{ pixel}^{-1}$ (50% probability in 1000 sec). This probability is a conservative upper limit. Rauscher et al. (2000) quote a $2 \times 10^{-4} \text{ sec}^{-1} \text{ pixel}^{-1}$ (20% probability in 1000 sec) cosmic ray hit probability. We have used the higher hit rate to ensure that the algorithm is robust to better than likely needed. The results of this work are not sensitive to this level of variation in the cosmic ray hit probability.

Each simulation run was done using an input source flux and with a random source position. The random source position was bounded to be within 1 pixel of the central position.

Four different image generation algorithms were tested.

1. Standard: This method generates two difference images from frames 2-4. The 1st frame is rejected due to possible reset transients. The minimum of the two difference images is chosen as the slope measurement on a pixel-by-pixel basis. This method was developed for bright targets with short exposure times, which will be the most common case.
2. Modified Standard: This method is similar to the previous, but is for use when longer exposures times are required. The number of frames collected is a multiple of 4. Four mega-frames are constructed by coadding the individual frames in 4 equal sized bins. The resulting 4 mega-frames are then used in the standard method described previously. See Figure 1 for an illustration of this method.

Check with the JWST SOCCER Database at: <http://soccer.stsci.edu/DmsProdAgile/PLMServlet>
To verify that this is the current version.

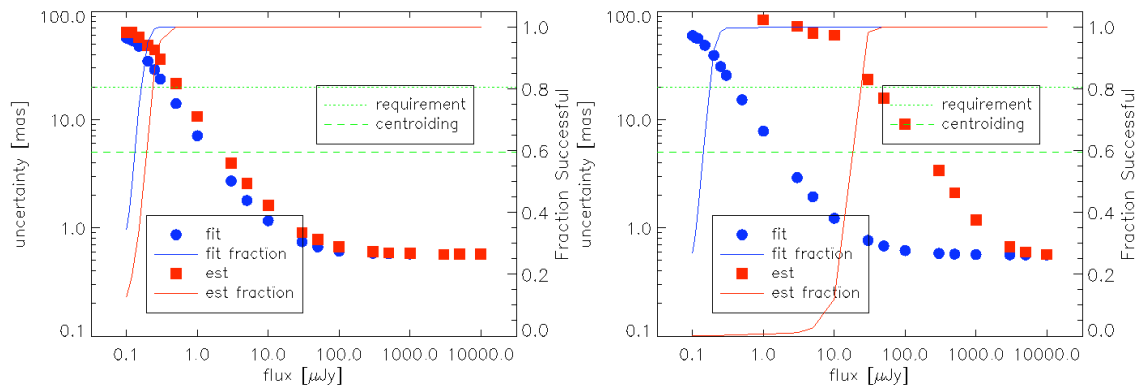


Figure 2: The radial centroiding accuracy as a function of source flux is shown for the full (solid blue circles, labeled fit) and modified (solid red squares, labeled est) methods. The simulations used to generate the left plot did not include cosmic rays while the simulations for the right plot did. The fraction of successful centroids (defined as measuring a centroid within 1 pixel [0.11"] of the correct position) is shown with the solid lines. The required accuracy is shown as a dotted green line and the required centroiding accuracy necessary to achieve this accuracy (accounting for the telescope small

3. Enhanced Standard: This method overcomes the drawbacks of the modified standard method for long exposures found in this study. Like the modified standard method the number of frames collected is a multiple of 4. The total number of frames is split into 4 sections. For each section, the slope is estimated by taking the max minus the min divided by the number of frames minus 1 ($n-1$) in the section. This results in 3 slope estimates for each pixel. Again, the 1st slope estimate is rejected due to possible reset transients. The minimum of the 3 slope estimates is used as the slope measurement. See Figure 1 for an illustration of this method.

4. Full: This method is the full solution that is similar to what will be done for the ground processing of the data. First, cosmic rays are identified using difference images for all pairs of consecutive frames in the ramp and doing an iterative sigma rejection. In the analysis presented here, the slope is determined by performing a linear least squares fit to the largest contiguous segment without a cosmic ray. This method approximates the best possible slope measurement, which will combine slope measurements for all segments.

There is a modification to the enhanced method that would make it more optimal without adding significant complexity. That would be to take 1 extra frame (e.g., 33). Then the reset transients could be removed by rejecting the first frame only (not $\frac{1}{4}$ of the integration) and 4 independent slope estimates determined. This would mean this method is robust to up to 3 cosmic rays. The nominal probability of 3 cosmic rays affecting any pixel in a 1000 second exposure is 0.000244 (0.0244%).

Check with the JWST SOCCER Database at: <http://soccer.stsci.edu/DmsProdAgile/PLMServlet>
To verify that this is the current version.

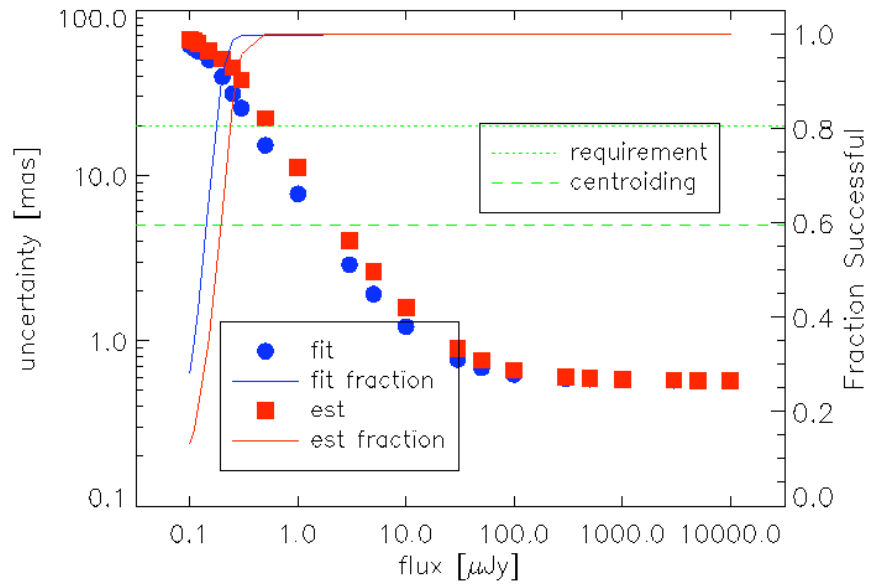


Figure 3: The radial centroiding accuracy as a function of source flux is shown for the full (solid blue circles, labeled fit) and enhanced (solid red squares, labeled est) methods. Cosmic rays were included in these simulations. The fraction of successful centroids (defined as measuring a centroid within 1 pixel (0.11”) of the correct position) is shown with the solid lines. The required accuracy is shown as a dotted green line and the required centroiding accuracy necessary to achieve this accuracy (accounting for the telescope small angle maneuver error) is shown as a dashed green line.

As can be seen from Figure 2, the modified method fails in the presence of cosmic rays. The reason for this is illustrated in Figure 1 where the cosmic ray corrupts the middle mega-frame. This then corrupts both slope measurements and, therefore, the slope estimate for this method does not clean out all the cosmic rays leading to a high failure rate of the centroiding algorithm.

Check with the JWST SOCCER Database at: <http://soccer.stsci.edu/DmsProdAgile/PLMServlet>
 To verify that this is the current version.

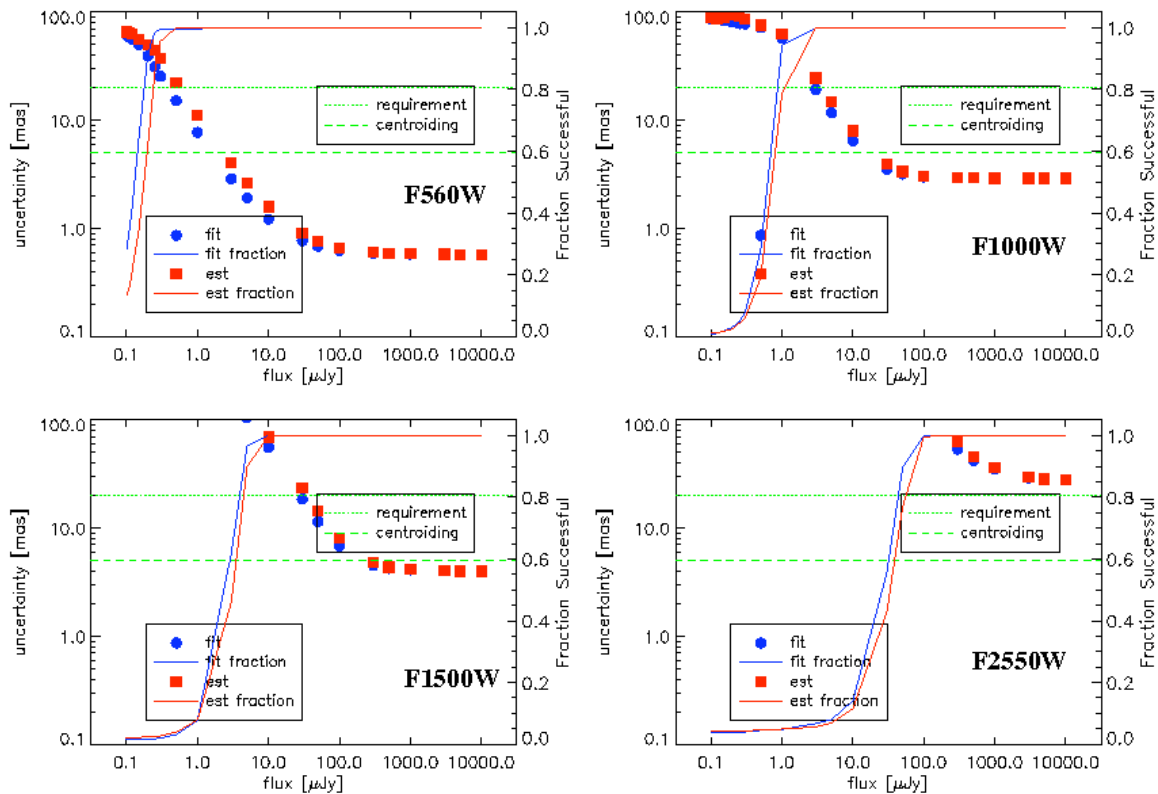


Figure 4: The radial centroiding accuracy is shown for the F560W, F1000W, F1500W, and F2550W filters for nominal sky levels. The details of these plots are the same as Fig. 3.

The results for the enhanced (#3) method as compared to the full (#4) method are shown in Figure 3. The enhanced method has similar centroiding accuracy to the full method even with cosmic rays present in the simulation. The reason for this is illustrated in Figure 1. The enhanced method uses 3 independent slope measurements to determine the final slope estimate. A cosmic ray hitting in one of the 3 segments used only corrupts that segment, leaving the other two slope measurements uncorrupted.

Check with the JWST SOCCER Database at: <http://soccer.stsci.edu/DmsProdAgile/PLMServlet>
To verify that this is the current version.

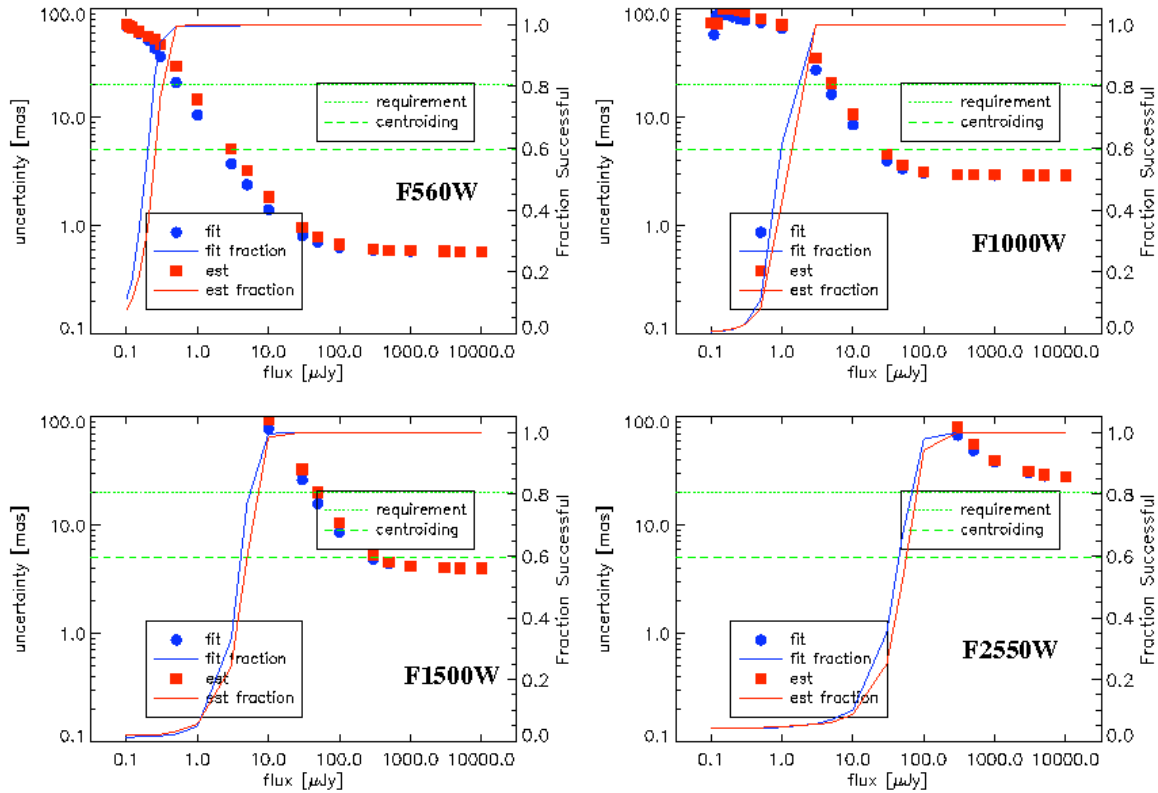


Figure 5: The radial centroiding accuracy is shown for the F560W, F1000W, F1500W, and F2550W filters for twice the nominal sky levels. The details of these plots are the same as Fig. 3.

4.2 Flux Limits

The simulations can be used to determine the minimum flux for the target acquisition source that allows for the required centroiding accuracy to be met. The value for the F560W filter with nominal sky level can be determined directly from Figure 3 to be $\sim 0.5 \mu\text{Jy}$. The sky level is expected to vary and thus it is useful to determine how much the sky level will affect the minimum flux level. Simulations for the F560W filter with 2x the nominal sky level give a very similar minimum flux of $\sim 0.5 \mu\text{Jy}$.

The sky level increases at longer wavelengths and some sources may be brighter at longer MIRI wavelengths. Thus, it is important to determine what the flux limits are for other MIRI filters and their dependence on sky brightness. The simulations were done for 3 other MIRI filters: F1000W, F1500W, and F2550W. The floating 1st moment centroid method window was 5x5, 7x7, and 9x9 pixels. The results are shown in Figures 4 & 5 and Table 2. Changing the sky level by a factor of two does not significantly affect the centroiding accuracy.

Table 2: Minimum Source Flux Required [in μJy]

	F560W	F1000W	F1500W	F2550W
Nominal sky/telescope level	2.7	25	288	X
2x sky/telescope level	3.1	28	379	X

1 to verify that this is the current version.

5.0 Conclusions

Target acquisition with faint sources can be done using long exposures (e.g. 1000 sec), but requires an enhanced method for the slope image creation to remove the numerous cosmic rays. The enhanced method creates independent slope estimates in subsections of the full exposure ramps and the minimum of these independent slope estimates is taken as the slope measurement. The faintest source for which a 5 mas or better centroid can be measured in 960 sec using the enhanced method was determined using simulations to be 2.7, 25, and 288 μ Jy for the F560W, F1000W, and F1500W filters, respectively. It is not possible to measure a 5 mas or better centroid with the F2550W filter. The use of this enhanced method for the slope image creation can be predicted based on the target acquisition flux level (i.e., it is not necessary for the user to specify which algorithm to use).

6.0 References

- Anandakrishnan, S. et al. 2006, NGST, DRD#D36177, Rev. B, "JWST Pointing Error Allocation and Performance Prediction Analysis"
- Glasse, A. 2006, MIRI-RP-00027-ATC, "The MIRI Calibration Error Budget"
- Meixner, M., Cavarroc, C., Regan, M., & Boccaletti, A., 2007, JWST-STScI-001134, "Target Location Algorithms for the Mid-Infrared Instrument (MIRI)"
- Rauscher, B. J., Isaacs, J. C., & Long, K. 2000, STScI-NGST-R-0003A, "Cosmic Ray Management on NGST 1: The Effects of Cosmic Rays on Near Infrared Imaging Exposure Times"